BULLETIN OF MATHEMATICS AND STATISTICS RESEARCH
A Peer Reviewed International Journal,
Contents available on www.bomsr.com
Vol.4. S1.2016; ISSN: 2348-0580
Email:editorbomsr@gmail.com
RADMAS– 2016

INFLUENCE OF VISCOUS DISSIPATION AND HEAT SOURCE ON MHD NANOFLUID FLOW AND HEAT TRANSFER TOWARDS A NONLINEAR PERMEABLE STRETCHING SHEET

SRINIVASASAI PANUGANTI[1], MUDDA RAMESH[2], GNANESWARA REDDY MACHIREDDY[3], PADMA POLARAPU[4]
[1,2,3]Department of Mathematics, ANU Ongole Campus, Ongole, A.P, India-523 001.
[4]Department of Mathematics,S.R.Govt.Arts&Science college,Kothagudem,Khammam,Telangana-507101
p.srinivasasai@gmail.com,mudda_ramesh@yahoo.com,mgrmaths@gmail.com,padmapolarapu@gmail.com

ABSTRACT
A numerical analysis has been presented on free convective boundary layer flow of a nanofluid along a non-linear permeable stretching sheet in the existence of viscous dissipation and internal heat generation. We have included the Brownian motion and thermophoresis effects. A suitable similarity transmutation is used to transform the governing equations into non-linear ordinary differential equations. A second order finite difference model known as Keller-Box method is used to solve numerically the governing boundary layer equations. The present mathematical values have been compared with the previously published values and good agreement is found. The impacts of various emerging parameters on velocity profiles, temperature and concentration profiles are presented graphically and mathematical results of reduced Nusselt number, skin fraction coefficient and the Sherwood numbers are presented in tabular form and graphs. An increase in the viscous dissipation parameter enhances the temperature and declines the concentration. The heat generation parameter enhances the skin friction coefficient. The effect of increasing the values of chemical reaction parameter is to decrease the concentration profiles. We made a conclusion that the rate of mass transfer enhances for rise of the chemical reaction parameter,

KEYWORDS: Nanofluid, Flow and heat transfer, Nonlinear permeable stretching sheet.

B_0	applied magnetic field
C	concentration of the nanofluid
C_f	skin friction coefficient
Cf_x	reduced skin friction coefficient
C_p	specific heat at constant pressure
C_W	concentration of the nanofluid along the stretching sheet
C_∞	ambient concentration
D_B	brownian diffusion coefficient
D_T	thermophoresis coefficient
E_C	viscous dissipation parameter
f	dimensionless stream function
g	acceleration due to gravity
Gr	local thermal Grashof number
Gm	local mass Grashof number
k	thermal conductivity of the fluid
k_e	mean absorption coefficient
k_p	permeability of the porous medium
Le	lewis number
M	magnetic parameter
Nb	brownian motion parameter
Nt	thermophoresis parameter
Nr	thermal radiation parameter
Nu	nusselt number
Nu_x	reduced nusselt number
Pr	prandtl number
q_r	radiative heat flux
q_m	mass flux
q_w	heat flux
R	thermal radiation parameter
Re_x	reynolds number
$R1^{-1}$	permeability parameter,
Sh	sherwood number
Sh_x	reduced sherwood number
T	fluid temperature
T_W	temperature of the nanofluid along the stretching sheet

BULLETIN OF MATHEMATICS AND STATISTICS RESEARCH
A Peer Reviewed International Journal,
Contents available on www.bomsr.com
RADMAS– 2016
Vol.4. S1.2016; ISSN: 2348-0580
Email:editorbomsr@gmail.com

T_∞	temperature of the fluid far away from the sheet	ρ_f	density of the base fluid
u	velocity in x direction	μ	dynamic viscosity
U_W	velocity of the stretching surface	ψ	stream function
U_0	uniform velocity	σ_s	stephan- Boltzmann constant
v	velocity in y direction	τ	ratio between the effective heat capacity of the nanoparticles and the fluid
x	horizontal distance	τ_W	shear stress
y	vertical distance	θ	dimensionless temperature variable
α	thermal diffusivity parameter	ϕ	dimensionless rescaled nanoparticle volume fraction
η	similarity variable	λ	buoyancy parameter
υ	kinematic viscosity	δ	solutal buoyancy parameter
β	thermal expansion coefficient	γ	heat source/sink parameter
β_c	coefficient of volumetric concentration Expansion	n, n_1	constants
β_T	coefficient of volumetric thermal expansion	m	stretching parameter

1. INTRODUCTION

A fluid which contains nanometer sized particles, called nanoparticles and a base fluid is called a nanofluid. The nanoparticles used in nanofluids are generally made of Carbides, Metals, Oxides, Nitrides or nonmetals (Carbon nanotubes, Graphite) and the base conductive fluid is a fluid, like water, ethylene glycol, toluene and oil. Studies related to nanofluids gave much interest in recent time due to their excessive enhanced performance properties, particularly with respect to the transfer of heat. Nanofluids have new properties that make them potentially useful in many advantages in heat transfer, including fuel cells, microelectronics, pharmaceutical processes and hybrid-powered engines. A great scientific interest is created in Nanoparticles since it is an effectively bridge between bulk materials and atomic or molecular structures. The technique of mixing nanoparticles and the base fluid was first proposed by Choi (1995). Later Das et al. (2003) showed experimentally a two-to four-fold raise in thermal conductivity enrichment for water based nanofluids containing Al_2O_3 or Copper nanoparticles over a small temperature range 210–510C. A satisfactory report for the abnormal increase of the thermal conductivity was given by Buongiorno (2006). Buongiorno and Hu (2005), investigated on the nanofluid coolants in advanced nuclear systems. Mixed convection boundary layer flow through a vertical flat plate filled with nanofluids and enclosed in a porous medium was inspected by Ahmad and Pop (2010). Hady et al. (2012) inspected the impacts of radiation on the flow and heat transfer of a nanofluid past a non-linearly stretching sheet. Olanrewaju and Olanrewaju et al. (2012) examined the impacts of radiation on the boundary layer flow of nanofluids past a moving surface. Hamid et al. (2011) analyzed the impacts of radiation on Marangoni boundary layer flow over a flat plate in a nanofluid. El-Aziz (2009) studied radiation effect on the flow and heat transfer over an unsteady stretching surface. Singh et al. (2010) investigated the thermal radiation and magnetic field impacts on an unsteady stretching permeable sheet in the existence of free stream velocity. Gbadeyan et al. (2011) studied the boundary layer flow of a nanofluid over a stretching sheet with convective boundary conditions in the existence of magnetic field and thermal radiation. Manna et al. (2012) studied the influence of radiation on unsteady MHD free convective flow over an oscillating vertical porous plate.

Magneto hydrodynamics (MHD) is the study of the interrelation of conducting fluids with electromagnetic incident. The flow of an electrically conducting fluid in the existence of a magnetic

BULLETIN OF MATHEMATICS AND STATISTICS RESEARCH
A Peer Reviewed International Journal,
Contents available on www.bomsr.com
RADMAS– 2016
Vol.4. S1.2016; ISSN: 2348-0580
Email:editorbomsr@gmail.com

field is of importance in different areas of engineering and technology such as MHD power generation, MHD pumps, MHD flow meters, etc. The study of MHD boundary layer flow on a continuous stretching sheet has pulled attention during the last few decades because of its various appliances in industrial manufacturing techniques. In particular the metallurgical processes such as tinning of copper wires, drawing and annealing involve cooling of continuous strips or filaments by drawing them through a quiescent fluid. Deformation and flow of materials require energy. The mechanical energy is dissipated, i.e. during the fluid flow it is converted into internal energy (heat) of the material. The increase of internal energy expresses itself on temperature rise. Viscous dissipation alters the temperature distributions by playing a role like an energy source, which leads to influence heat transfer rates. The merit of the effect of viscous dissipation depends on whether the plate is being cooled or heated. Viscous dissipation is of interest of many applications. Significant temperature increments are detected in polymer processing flows such as injection molding or extrusion at high rates. Aerodynamic heating in the thin boundary layer over high speed aircraft increases the temperature of the skin. In a completely different purpose, the dissipation function is utilized to define the viscosity of dilute suspensions (Einstein 1906, 1911): viscous dissipation for a fluid with appended particles is equated to the viscous dissipation in a pure Newtonian fluid both exist in the same flow. It is now well accepted fact that the terms magneto hydrodynamics (MHD) heat generation and thermal radiation broadly appear in various engineering processes. MHD is significant in the control of boundary layer flow and metallurgical procedures. The thermal radiation and heat generation possessions may results in high temperature factors processing operations. Ingredients may be intelligently arranged therefore with judicious implementation of radiative heating to generate the required characteristics. This recurrently takes place in plasma studies, agriculture, engineering and petroleum industries. The investigation of heat generation or absorption in moving fluids is essential in problems dealing with chemical reactions and these concerned with disassociating fluids. Heat generation is also important in the content of exothermic or endothermic chemical reactions. The heat and mass transfer problems with chemical reaction are of useful in many procedures, and therefore have acquired a considerable amount of attention in recent years. In order to transform cheaper raw materials to high value products, the raw materials are made to go through chemical reaction in all industrial chemical procedures. Such chemical transformations exist in a reactor. The reactor plays an important act of bringing reactants into close contact and providing an proper environment for adequate time and allowing the dismissal of finished products. Thus we are especially interested in cases in which diffusion and chemical reaction roughly the same speed. In processes, like drying, vaporization at the surface of a water body, energy transfer in a wet cooling tower and the flow in desert cooler, groves of fruit trees, electric power generation; the heat and mass transmission take place simultaneously. In many chemical engineering procedures, a chemical reaction between a foreign mass and the fluid take place. These procedures take place in various industrial applications, such as the polymer construction, the manufacturing of ceramics or glassware, food processing. Most chemical reactions contain the breaking and formation of chemical bonds. It requires energy to break a chemical bond but energy is discharged when chemical bonds are formed.

BULLETIN OF MATHEMATICS AND STATISTICS RESEARCH
A Peer Reviewed International Journal,
Contents available on www.bomsr.com
RADMAS– 2016
Vol.4. S1.2016; ISSN: 2348-0580
Email:editorbomsr@gmail.com

Kuznetsov and Nield (2010) have investigated the impact of nanoparticles on the natural convection boundary layer flow towards a vertical plate integrating the Brownian motion and Thermophoresis treating both the temperature and the nanoparticles fraction as stable along the wall. Further, Nield and Kuznetsov (2009) have studied the problem proposed by Cheng and Minkowycz (1977) about the natural convection over a vertical plate in porous medium saturated by a nanofluid integrating the Brownian motion and thermophoresis. All these researchers studied linear stretching sheet in the nanofluid, but a numerical research was done by Rana and Bhargava (2011) who studied the steady laminar boundary fluid flow of nanofluid past a nonlinear stretching flat surface with the combined impacts of Brownian motion and thermoporesis. Fazlul Kader Murshed et al. (2015) extended the work of Rana and Bhargava by taking thermal radiation on boundary layer flow of a nanofluid towards a nonlinearly permeable stretching sheet. Also recently Nadeem and Lee (2012) investigated analytically the problem of steady boundary layer flow of nanofluid over an exponentially `widening surface including the effects Brownian motion parameter and thermophoresis parameter. Investigations were done on dual solutions of radiative MHD nanofluid flow past an exponentially unfolding sheet with heat generation/absorption (2015). Khan and Pop (2010) investigated the boundary layer flow of a nanofluid past a stretching sheet. Makinde and Olanrewaju (2010) examined the buoyancy impacts on thermal boundary layer past a erecting plate with a convective boundary condition. Gnaneswara Reddy (2014) examined the thermal radiation and chemical reaction impacts on MHD mixed convective boundary layer slip flow in a porous medium with ohmic heating and heat source. Gnaneswara Reddy (2014) examined the impacts of viscous dissipation, thermal radiation and hall current on MHD convection flow over a unfold vertical flat plate. It was found that the velocity, cross flow velocity and temperature distribution raises as the radiation parameter or viscous dissipation parameter increases. Gnaneswara Reddy (2014) investigated the impacts of Thermophoresis, viscous dissipation and joule heating on steady MHD flow over an inclined radiative isothermal porous surface with variable thermal conductivity. Gnaneswara Reddy et al. (2015) studied the impacts of viscous dissipation and heat source on unsteady MHD flow over a stretching sheet.

But so far, no contribution is made with the impacts of viscous dissipation, permeability heat source and chemical reaction parameter on heat and mass transfer of MHD free convective boundary layer flow towards a nonlinear stretching sheet and hence the present work is carried out due to its abundant applications. So the aim of present paper is to study the simultaneous impacts of viscous dissipation, internal heat generation, chemical reaction on magneto hydro dynamic flow and heat transfer of nanofluids through porous medium over a non-linear stretching sheet. The governing boundary layer equations are reduced to a combination of nonlinear ordinary differential equations using similarity transmutations. By using Keller box method the nonlinear ordinary differential equations are settled mathematically. A parametric study is conducted to illustrate the impacts of various governing parameters on the velocity profiles, temperature distribution, concentration profiles, local Nusselt number, Skin friction coefficient and Sherwood number are discussed in detail.

2. FORMULATION OF THE PROBLEM

We consider a steady, laminar, incompressible, two-dimensional boundary layer flow of a viscous

RADMAS– 2016

BULLETIN OF MATHEMATICS AND STATISTICS RESEARCH

A Peer Reviewed International Journal,

Contents available on www.bomsr.com

Vol.4. S1.2016; ISSN: 2348-0580

Email:editorbomsr@gmail.com

water based nanofluids over a stretching sheet coinciding with the plane $y = 0$ and the flow being restricted to $y > 0$. The flow is created in view of nonlinear stretching of the sheet caused by the simultaneous application of two equal and opposite forces along the x -axis. Fixing the origin, the sheet is then stretched with a velocity $U_w(x) = U_0 x^m$ where U_0 is the uniform velocity. m ($m \geq 0$) is a constant parameter. The fluid is considered to be a gray, absorbing emanating radiation but non scattering medium. The flow is subjected to a uniform transverse magnetic field of strength $B = B_0$ which is applied in the positive y-direction, normal to the surface. The fluid is assumed to be slightly conducting, so that the magnetic Reynolds number is supposed to be small so that the induced magnetic field is negligible in comparison to the applied magnetic field. It is supposed that the porous medium is homogeneous and present everywhere in local thermodynamic equilibrium. The remaining properties of the fluid and the porous medium are assumed to be constant. Both the base fluid and the nanoparticles are supposed to be in thermal equilibrium and no slip occurs between them. The Hall Effect is also negligible. The pressure gradient and external forces are neglected. A schematic model of the problem under consideration is depicted in Fig. 1. Under the above assumptions, and employing the Oberbeck- Boussinesq approximation, the emerging equations of the flow field in presence of viscous dissipation, heat source and porous medium can be written in the dimensional form as

$$\frac{\partial u}{\partial x} + \frac{\partial u}{\partial y} = 0 \qquad (1)$$

$$\frac{\partial p}{\partial x} - \mu \frac{\partial^2 p}{\partial y^2} = \rho_f \left(u \frac{\partial u}{\partial x} + v \frac{\partial u}{\partial y} \right)$$
$$\begin{bmatrix} (1 - C_\infty)\rho_{f_\infty}\beta_T (T - T_\infty) - \\ (\rho_p - \rho_{f_\infty})\beta_C (C - C_\infty) \end{bmatrix} g - B_0^2 u - \frac{\mu}{\rho}\frac{u}{k_p} \qquad (2)$$

$$u \frac{\partial T}{\partial x} + v \frac{\partial T}{\partial y} = \alpha \nabla^2 T + \tau \left\{ D_B \left(\frac{\partial T}{\partial y} \frac{\partial C}{\partial y} \right) \frac{D_T}{T_\infty} \left(\frac{\partial T}{\partial x} \right)^2 \right\}$$
$$- \frac{1}{(\rho C_p)_f} \frac{\partial q_r}{\partial y} + \frac{Q}{\rho c_p}(T - T_\infty) + \frac{\mu}{\rho c_p}\left(\frac{\partial u}{\partial y} \right)^2 \qquad (3)$$

$$u \frac{\partial C}{\partial x} + v \frac{\partial C}{\partial y} = D_B \frac{\partial^2 C}{\partial y^2} + \frac{D_T}{T_\infty} \frac{\partial^2 T}{\partial y^2} - k_r (C - C_\infty) \qquad (4)$$

where u and v are the velocities in the x and y-directions, respectively, g is the acceleration due to gravity, μ-the viscosity, ρ_f-the density of the base fluid, ρ-the density of the nanoparticle, β_T-the coefficient of volumetric thermal expansion, β_C-the coefficient of volumetric concentration expansion, T-the temperature of the nanofluid, C-the concentration of the nanofluid, T_w and C_w-the temperature and concentration along the stretching sheet, T_∞ and C_∞-the ambient temperature and concentration , D_B- the Brownian diffusion coefficient, D_T-the thermophoresis coefficient, B_0-the magnetic induction, q_r-radiative heat flux, k-the thermal conductivity, $(\rho C)_p$-the heat capacitance of the nanoparticles, $(\rho C)_f$-the heat capacitance of the base fluid, k_p-the permeability of the porous medium, Q-the volumetric rate of heat generation/absorption, $\alpha = k/(\rho C)_f$ is the thermal diffusivity parameter and $\tau = (\rho C)_p/(\rho C)_f$ is the ratio between the effective heat capacity of the nanoparticles material and heat capacity of the fluid.

The associated boundary conditions are

RADMAS– 2016

BULLETIN OF MATHEMATICS AND STATISTICS RESEARCH
A Peer Reviewed International Journal,
Contents available on www.bomsr.com
Vol.4. S1.2016; ISSN: 2348-0580
Email:editorbomsr@gmail.com

$$u \to 0, v \to 0, T \to T_\infty, C \to C_\infty \ as\ y \to \infty$$

s $$u = U_0 x^m, \mathrm{v} = 0, \mathrm{T} = T_w, C = C_w \ at\ y = 0 \quad (5)$$

By using the Rosseland approximation (1992), the radiative heat flux q_r is given by

$$q_r = \frac{-4\sigma_s}{3k_e}\frac{\partial T^4}{\partial y} \qquad (6)$$

where σ_s is the Stephen Boltzmann constant and k_e is the mean absorption coefficient.

It should be noted that by using the Rosseland approximation, the present analysis is limited to optically thick fluids. If the temperature differences within the flow are sufficiently small, then equation (6) can be linearised by expanding T^4 into the Taylor series about T_∞, which after neglecting higher order terms takes the form

$$\mathrm{T}^4 \cong 4\mathrm{T}^3_\infty \mathrm{T} - 3\mathrm{T}_\infty{}^4 \qquad (7)$$

Then the radiation term in equation (3) takes the form

$$\frac{\partial q_r}{\partial y} = \frac{16\sigma_s T_\infty^3}{3k_e}\frac{\partial^2 T^4}{\partial y^2} \qquad (8)$$

Invoking equation (8), equation (3) gets modified as

$$u\frac{\partial T}{\partial x} + v\frac{\partial T}{\partial y} = \left(\frac{k}{(\rho C_p)_f} + \frac{16\sigma_s T_\infty^3}{3k_e(\rho C_p)_f}\right)\frac{\partial^2 T}{\partial y^2} \qquad (9)$$
$$+\tau\left\{D_B\left(\frac{\partial T}{\partial y}\frac{\partial C}{\partial y}\right)\frac{D_T}{T_\infty}\left(\frac{\partial T}{\partial x}\right)^2\right\} + \frac{Q}{\rho c_p}(T - T_\infty) + \frac{\mu}{\rho c_p}\left(\frac{\partial u}{\partial y}\right)^2$$

Let we introduce a stream function $\psi(x, y)$ in the flow field such that $u = \frac{\partial \psi}{\partial y}$, $v = -\left(\frac{\partial \psi}{\partial x}\right)$. It is obvious that the equation of continuity (1) is satisfied.

Assuming that the external pressure on the plate, in the direction having diluted nanoparticles, to be constant, the similarity transformations are taken as

$$\psi = \sqrt{\frac{2\upsilon U_0 x^{m+1}}{m+1}} f(\eta), \theta(\eta) = \frac{T - T_\infty}{T_w - T_\infty}, \ \phi(\eta) = \frac{C - C_\infty}{C_w - C_\infty},$$

$$\eta = y\sqrt{\frac{(m+1)U_0 x^{m-1}}{2\upsilon}}, Nr = \frac{k_e k}{4\sigma_s \mathrm{T}^3_\infty}, R = \frac{4}{3Nr}, \lambda = \frac{Gr}{Re_x^{\frac{3}{2}}},$$

$$\delta = \frac{Gm}{Re_x^{\frac{3}{2}}}, \Pr = \frac{\upsilon}{\alpha}, Le = \frac{\upsilon}{D_B}, \upsilon = \frac{\mu}{\rho_f}, Nb = \frac{\tau D_B}{\upsilon}(C_w - \mathrm{C}_\infty),$$

$$Nt = \frac{\tau D_T}{\upsilon \mathrm{T}_\infty}((T_w - \mathrm{T}_\infty)), Re_x = \frac{u_w(x)x}{\upsilon}, Gr = \frac{(1 - \mathrm{C}_\infty)\left(\frac{\rho_{f\infty}}{\rho_f}\right) gn(T_w - \mathrm{T}_\infty)}{\upsilon^2 Re_x^{\frac{1}{2}}},$$

$$Gm = \frac{\left(\frac{\rho_p \rho_{f\infty}}{\rho_f}\right) gn_1(C_w - \mathrm{C}_\infty)}{\upsilon^2 Re_x^{\frac{1}{2}}}, M = \frac{2\sigma B^2}{\rho_f U_0 (m+1) x^{m-1}}, R_1 = \frac{k(m+1)U_0 x^{m-1}}{2\upsilon},$$

$$Ec = \frac{U_0{}^2 x^{2m}}{c_p(T_w - T_\infty)}, \gamma = \frac{2Q}{(m+1)\rho_{c_p} U_0 x^{m-1}}, \gamma_1 = \frac{2k_r}{(m+1)U_0 x^{m-1}} \qquad (10)$$

BULLETIN OF MATHEMATICS AND STATISTICS RESEARCH
A Peer Reviewed International Journal,
Contents available on www.bomsr.com
RADMAS– 2016
Vol.4. S1.2016; ISSN: 2348-0580
Email:editorbomsr@gmail.com

Using the similarity transformations, the governing equations (2) – (4) are transformed to the nonlinear differential equations,

$$f''' + ff'' - \frac{2m}{m+1} f'^2 + \frac{2}{m+1}(\lambda\theta - \delta\phi) - Mf' - R_1^{-1} f' = 0 \qquad (11)$$

$$\frac{1}{\Pr}(1+R)\theta'' + f\theta' + Nb\theta'\phi' + Nt\theta'^2 + Ecf''^2 + \gamma\theta = 0 \qquad (12)$$

$$\phi'' + Lef\phi' + \frac{Nt}{Nb}\theta'' - Le\gamma_1\phi = 0 \qquad (13)$$

where λ- the buoyancy parameter, δ-the solutal buoyancy parameter, Pr-the Prandtl number, Le-the Lewis number, υ-the kinematic viscosity of the fluid, Nb-the Brownian motion parameter, Nt-the thermophoresis parameter, Re_x-the local Reynolds number based on the stretching velocity, Gr-the local thermal Grashof number, Gm-the local concentration Grashof number, M-the magnetic parameter, $R1^{-1}$-the permeability parameter, R-the radiation parameter, Ec-the Eckert number, γ-the heat source parameter $\gamma_1 = \frac{2k_r}{(m+1)U_0 x^{m-1}}$-the chemical reaction parameter and $f,\ \theta,\ \phi$ are the dimensionless stream functions, temperature, rescaled nanoparticle volume fraction respectively. Here, β_T and β_C are proportional to x^{-3}, that is $\beta_T = nx^{-3}$and $\beta_C = n_1 x^{-3}$, where n and n_1 are the constants of proportionality (Makinde and Olanrewaju, (2010).

The corresponding boundary conditions are

$$\begin{aligned} &f = 0,\ f' = 1, \theta = 1, \phi = 1 \quad at \quad \eta = 0 \\ &f' \to 0, \theta \to 0, \phi \to 0 \quad as \quad \eta \to \infty \end{aligned} \qquad (14)$$

Now, we are interested to study the quantities of practical interest, the skin friction coefficient C_f and the local Nusselt number Nu, Sherwood number Sh. The parameters respectively, characterize the surface drag, wall heat transfer rate and mass transfer rate. These quantities are defined by:

$$\begin{aligned} C_f &= \frac{2\tau_w}{\rho U^2} = \frac{2\mu}{\rho U_0^2}\left(\frac{\partial u}{\partial y}\right)_{y=0} \\ &= \frac{1}{\sqrt{2(m+1)}} Re_x^{\frac{1}{2}} f''(0) \end{aligned} \qquad (15)$$

$$\begin{aligned} Nu &= \frac{q_w x}{k(T_w - T_\infty)} = -\frac{q_w}{(T_w - T_\infty)} \\ \left(\frac{\partial T}{\partial y}\right)_{y=0} &= -\sqrt{\frac{2}{(m+1)}} Re_x^{-1/2}\theta'(0) \end{aligned} \qquad (16)$$

BULLETIN OF MATHEMATICS AND STATISTICS RESEARCH
A Peer Reviewed International Journal,
Contents available on www.bomsr.com
Vol.4. S1.2016; ISSN: 2348-0580
Email:editorbomsr@gmail.com
RADMAS– 2016

$$Sh = \frac{q_m x}{k(C_w - C_\infty)} = -\frac{q_m}{(C_w - C_\infty)}$$
$$\left(\frac{\partial C}{\partial y}\right)_{y=0} \quad S = -\sqrt{\frac{2}{(m+1)}} Re_x^{-1/2} \varphi'(0) \tag{17}$$

3. NUMERICAL SOLUTION

Since equations (11) – (13) are highly non-linear, it is difficult to find the closed form solutions. Keller Box method (1912, 1974) is used to solve these equations with the boundary conditions (14). The numerical values of local Nusselt number, Skin friction coefficient and local Sherwood number are presented in tabular form.

4. RESULTS AND DISCUSSION

To get a physical insight into the flow problem, comprehensive numerical computations are conducted for various values of emerging parameters that describe the flow characteristics and the results are illustrated graphically. The value of Pr is taken as 0.71 which corresponds to air. The values of Sc are chosen such that they represent Helium (0.3), water vapor (0.62) and Ammonia (0.78). The other parameters are chosen arbitrarily. The present results are compared with that of Khan and Pop (2010), Anwar et al. (2012) and got an excellent agreement. Keller Box method is used to solve the resulting nonlinear ordinary differential equations (11) – (13) subject to the boundary conditions (14). Velocity, temperature and concentration profiles were obtained and we applied the results to calculate the skin friction coefficient, the local Nusselt number and the local Sherwood number in equations (15), (16) and (17). The accuracy of the method depends on the choice of the appropriate initial guesses. We have taken the following initial guesses :

$f_0(\eta) = 1 - e^{-\eta}, \theta_0(\eta) = e^{-\eta}, \phi_0(\eta) = e^{-\eta}$ (18) The choices of the above suitable initial guesses depend on the convergence criteria and the wall shear stress $f''(0)$ is commonly used as a convergence criterion because in the boundary layer flow calculations the greatest error appears in the wall shear stress parameter as it is mentioned in the book by Cebeci and Bradshaw (1988). Thus, we used this convergence criterion in the present study. A uniform grid of size 0.004 is chosen to satisfy the convergence criterion of 10^{-7} in our study, which gives about six decimal places accurate to most of the prescribed quantities. From the process of numerical computation, the numerical values of the local Nusselt number, Skin friction coefficients and Sherwood number are represented in tabular form.

The impacts of various emerging parameters on the Skin friction coefficient $f''(0)$, Nusslet number $-\theta'(0)$ and Sherwood number $-\phi'(0)$ are shown in Table 1. It is observed that as $M, R1^{-1}, Nt, m$ or δ increaes all the three Skin friction coefficient, Nusslet number and Sherwood number declines. As Le or λ increases then the Nusselt number, Skin friction coefficient and Sherwood number rises. We came o he conclusion that the thermal radiation parameter R decreases both the Nusselt number, Skin friction coefficient and enhances the Sherwood number. An increase in the Eckert number Ec or Nb leads to a raise in the Skin friction coefficient and Sherwood number. An increase in the Eckert number Ec or Nb leads to a fall in the Nusslet number. When the values of Pr or γ_1 increase, both the Nusslet number and Sherwood number rise whereas the Skin friction coefficient

BULLETIN OF MATHEMATICS AND STATISTICS RESEARCH
A Peer Reviewed International Journal,
Contents available on www.bomsr.com
Vol.4. S1.2016; ISSN: 2348-0580
Email:editorbomsr@gmail.com
RADMAS– 2016

decreases. The numerical results are discussed for the values of the physical parameters graphically and in tabular form. The present results are compared with that of Khan and Pop (2010) and Anwar et al. (2012) in the absence of permeability, viscous dissipation and heat source and found that there is an excellent agreement (Table 2).

Table 1 Numerical values of the Skin friction coefficient, Nusselt number and the Sherwood number for various physical parameters.

M	R	Ec	Q	R_1	Pr	Nb	Nt	Le	m	δ	γ_1	λ	$-f''(0)$	$-\theta'(0)$	$-\varphi'(0)$
0.5	0.2	0.1	0.1	100	0.71	0.1	0.1	10	1	1	0.1	1	0.8763	0.3745	2.5068
1	0.2	0.1	0.1	100	0.71	0.1	0.1	10	1	1	0.1	1	1.0945	0.3497	2.4764
0.5	0.4	0.1	0.1	100	0.71	0.1	0.1	10	1	1	0.1	1	0.8641	0.3581	2.5138
0.5	0.2	0.2	0.1	100	0.71	0.1	0.1	10	1	1	0.1	1	0.8724	0.3579	2.5178
0.5	0.2	0.1	0.2	100	0.71	0.1	0.1	10	1	1	0.1	1	0.8567	0.3158	2.5406
0.5	0.2	0.1	0.1	150	0.71	0.1	0.1	10	1	1	0.1	1	0.8748	0.3747	2.5071
0.5	0.2	0.1	0.1	100	10	0.1	0.1	10	1	1	0.1	1	1.1548	0.5204	2.6154
0.5	0.2	0.1	0.1	100	0.71	0.3	0.1	10	1	1	0.1	1	0.8634	0.3372	2.5423
0.5	0.2	0.1	0.1	100	0.71	0.1	0.3	10	1	1	0.1	1	0.8905	0.3482	2.4653
0.5	0.2	0.1	0.1	100	0.71	0.1	0.1	15	1	1	0.1	1	0.8432	0.3767	3.1262
0.5	0.2	0.1	0.1	100	0.71	0.1	0.1	10	2	1	0.1	1	1.0854	0.3467	2.4754
0.5	0.2	0.1	0.1	100	0.71	0.1	0.1	10	1	2	0.1	1	1.0878	0.3649	2.4856
0.5	0.2	0.1	0.1	100	0.71	0.1	0.1	10	1	1	0.2	1	0.8691	0.3750	2.6977
0.5	0.2	0.1	0.1	100	0.71	0.1	0.1	10	1	1	0.1	2	0.3815	0.4257	2.5761

Table 2 Comparison of Reduced Nusselt number, Reduced Sherwood number with $\gamma = 0$

Nb	Nt	Pr	Le	λ	δ	M	Anwar & Khan et al. (2012)		Poornima & Reddy (2013)		Present results	
							$-\theta'(0)$	$-\phi'(0)$	$-\theta'(0)$	$-\phi'(0)$	$-\theta'(0)$	$-\phi'(0)$
0.1	0.1	10	10	0	0	1	0.9524	2.1294	0.952376	2.12939	0.952402	2.129444
0.2	0.2						0.3654	2.5152	0.365357	2.51522	0.365302	2.515377
0.3	0.3						0.1355	2.6088	0.135514	2.60881	0.135429	2.608999
0.4	0.4						0.0495	2.6038	0.049465	2.60384	0.49389	2.604008
0.5	0.5						0.0179	2.5731	0.017922	2.5731	0.017868	2.573240

Table 3 Computations of velocity and temperature profiles for different values of δ.

δ	$f'(\eta)$	$\theta(\eta)$	$f'(\eta)$	$\theta(\eta)$	$f'(\eta)$	$\theta(\eta)$
	$\eta = 1$		$\eta = 2$		$\eta = 3$	
1	0.9893191	0.9968845	0.9788352	0.9937519	0.9685441	0.9906027
2	0.9871958	0.9970185	0.9746858	0.9940174	0.9624634	0.9909972
3	0.9850163	0.9971677	0.9704243	0.9943126	0.9562146	0.9914354

Table 4 Computations of concentration profiles $\phi(\eta)$ for different values of M, R, λ and γ.

	$\phi(\eta)$			$\phi(\eta)$			$\phi(\eta)$			$\phi(\eta)$		
	M			R			λ			γ		
η	0.5	2.0	3.0	0.0	0.5	1.0	1.0	2.5	3.5	0.0	0.1	0.3
2	0.9539	0.9558	0.9565	0.9549	0.9544	0.9540	0.9546	0.9524	0.9511	0.9555	0.9546	0.9527
3	0.9310	0.9338	0.9353	0.9324	0.9316	0.9311	0.9321	0.9286	0.9267	0.9333	0.9321	0.9291

BULLETIN OF MATHEMATICS AND STATISTICS RESEARCH
A Peer Reviewed International Journal,
Contents available on www.bomsr.com
Vol.4. S1.2016; ISSN: 2348-0580
Email:editorbomsr@gmail.com
RADMAS– 2016

The effects of various governing parameters upon the nature of the flow and transport are discussed in detail. The numerical results are depicted graphically in Figs. 2 – 30. Unless otherwise mentioned, the default values are $Pr = 0.71$, $Le = 10$, $\lambda = 1$, $m = 1$, $M = 1$, $Nt = Nb = Ec = 0.1$, $R_1 = 100$, $R = 0.2$, $\gamma = 0.1$ $\gamma_1 = 0.1$ and $\delta = 1$ for our subsequent results.

The velocity profiles for various values of emerging parameters are elucidated in Figures 2–9. From these Figures it is observed that the fluid velocity is highest at the stretching porous sheet and decreases exponentially to its free stream zero value satisfying the far field boundary conditions. It is observed that the effect of increasing the values of Prandtl number, the stretching parameter m, magnetic parameter, heat source parameter and solutal buoyancy parameter is to decrease velocity profiles as illustrated in Figures 2-6, whereas a reverse trend is observed with increasing the values of buoyancy parameter, radiation parameter and the permeability parameter, which is clear from Figs.7-9. We define the Prandtl number Pr as the ratio of momentum diffusivity to thermal diffusivity. It is noticed that an increase in the Prandtl number makes the fluid to be more viscous, which leads to a decrease in the velocity (Fig. 2). When the magnetic parameter increases, the velocity profiles decrease. This is because, the application of the magnetic field within the boundary layer produces a Lorentz force which opposes the flow and decelerates the fluid motion which is clear from Fig. 4. The influence of the solutal buoyancy parameter, on velocity $f'(\eta)$ is shown in Figs. 6 and Table 3. It is noticed that a rise in solutal buoyancy parameter causes a decrease in velocity. The positive (+ve) buoyancy force acts like a supportive pressure gradient and hence accelerates the fluid in the boundary layer. This results in higher velocity as λ increases. The radiation parameter R defines the relative contribution of conduction heat transfer to thermal radiation transfer. It is clear from Fig. 8 that an increase in the radiation parameter results in increasing velocity within the boundary layer. As shown in Fig. 9 the effect of increasing the value of porous permeability is to raise the value of the velocity component in the boundary layer due to the fact that drag is reduced by increasing the value of porous permeability on the fluid flow which results in raised velocity.

The temperature profiles for various values of governing parameters are elucidated in Figures 10–20. From these Figures we made a conclusion that the fluid temperature is highest at the stretching porous sheet and decreases exponentially to its free stream zero value satisfying the far field boundary conditions. We have observed that the effect of increasing the values of Prandtl number, the buoyancy parameter and the Permeability parameter is to decrease temperatue as illustrated in Figures 10-12, whereas an opposite trend is observed with increasing the values of the stretching parameter m, radiation parameter, thermophoresis parameter, Brownian motion parameter, Eckert number, magnetic parameter, solutal buoyancy parameter and heat source parameter which is clear from Figs.13-20. Enhancing the Prandtl number results in a reduction in thermal diffusivity. We have noticed that the Fig. 10 temperature decreases with an increase in the Prandtl number. This results in reducing the thermal boundary layer thickness. The reason is that smaller values of Pr are equivalent to rising the thermal conductivities, and therefore heat is able to diffuse away from the heated stretching sheet more immediately than for higher values of Pr. Hence for higher values of Prandtl numbers, the boundary layer thickness decreases so the rate of heat transfer is increased. The radiation parameter R is responsible to thickening the thermal boundary layer. This enables the

BULLETIN OF MATHEMATICS AND STATISTICS RESEARCH
A Peer Reviewed International Journal,
Contents available on www.bomsr.com
Vol.4. S1.2016; ISSN: 2348-0580
Email:editorbomsr@gmail.com
RADMAS– 2016

fluid to release the heat energy from the flow region and causes the system to cool. This is true because increasing the Rosseland approximation results in an increase in temperature (1992). From Fig. 14 it is noticed that the radiation effect enhances temperature of the fluids and the absence of radiation defines small temperatures. Therefore, radiation enhances the buoyancy force. It is seen that the increase of the radiation parameter leads to decrease the boundary layer thickness and thereby decrease in the value of the heat transfer in the presence of thermal and solutal buoyancy force. Due to the larger values of Nt the thermophoretic forces are produced. These forces have the tendency to leave the nanoparticles in the reverse direction of temperature gradient (i.e., from hot to cool) which causes a non-uniform nanoparticle distribution. Consequently, the increasing values of Nt corresponds to an increase in the temperature. The Brownian motion is stronger in case of smaller nanoparticles which corresponds to the greater Nb and converse is the situation for smaller values of Nb. In thermal conduction nanoparticle's motion plays a pivotal role. Due to the increased chaotic motion of the nanoparticles (i.e., for larger b) the kinetic energy of the particle is enhanced which as a result enhances the temperature of the nanofluid. Hence increasing Nb firmly rises temperature values throughout the regime as illustrated in Fig. 16.An increase in viscous dissipation parameter Ec increases the temperature because the heat energy is stored in the liquid due to the frictional heating. The viscous dissipation parameter Ec expresses the relationship between the kinetic energy in the flow and the enthalphy [30]. It expresses the conversion of kinetic energy into internal energy by work done against the viscous fluid stresses. Larger viscous dissipative heat causes a rise in the temperature. This behavior is evident from Fig. 17. The positive value of viscous dissipation parameter Ec cools the sheet i.e., loss of heat from the sheet to the fluid. The influence of the solutal buoyancy parameter, on temperature $\theta(\eta)$ is shown in Fig. 19 and Table 3. It is observed that the temperature increases as the solutal buoyancy parameter increases. Fig. 20 has been plotted to depict the impact of heat source parameter on temperature profiles. From this Figure we observe that temperature increases with increase in the heat source parameter because when heat is released, the buoyancy force increases the temperature.

The concentration profiles are illustrated in Figures 21–29 for various values of emerging parameters. From these Figures it is observed that the fluid concentration is highest at the stretching porous sheet and reduces exponentially to its free stream zero value satisfying the far field boundary conditions. It is observed that the effect of increasing the values of thermophoresis parameter, the buoyancy parameter, the viscous dissipation parameter, Lewis number, heat source parameter radiation parameter and chemical reaction parameter is to decrease concentration profiles as illustrated in Figures 21-27, whereas a reverse trend is observed with increasing the values of Brownian motion parameter and magnetic parameter which is clear from Figs. 28-29. The impact of the thermal buoyancy parameter on the concentration field is shown in Fig. 22 and Table 4. It is noticed that the concentration decreases as the thermal buoyancy parameter increases. It is observed that the concentration decreases as the thermal buoyancy parameter increases. There would be a significant reduction in the concentration boundary layer thickness when Le is increased. This phenomenon occurs due to Lewis number effects which raises the concentration gradient at the surface, and as a result rises the local Sherwood number as elucidated in Fig. 24. Table 4 and Fig. 25

BULLETIN OF MATHEMATICS AND STATISTICS RESEARCH
A Peer Reviewed International Journal,
Contents available on www.bomsr.com
RADMAS– 2016
Vol.4. S1.2016; ISSN: 2348-0580
Email:editorbomsr@gmail.com

show the effect of the radiation parameter on the concentration. It is noticed that the concentration reduces as the radiation parameter enhances Table 4 and Fig. 26 show the effect of heat source parameter on the concentration profiles. It is observed that the concentration declines as γ increase. The effect of increasing the values of chemical reaction motion parameter is to decrease the concentration profiles as shown in Fig. 27. The effect of increasing the values of Brownian motion parameter is to increase the concentration profiles as shown in Fig. 28. The effect of the magnetic parameter on the concentration field is illustrated in Fig. 29 and Table 4. It is shown that a rise in the magnetic parameter causes an increase in the concentration.

The effects of the magnetic parameter and $R1$ on skin friction coefficient are shown in Fig. 30. This Figure indicates an increase in the values of skin friction coefficient with the increase in the values of magnetic parameter.

The following conclusions were drawn.

1. Velocity decelerates with an increase in the Prandtl number, solutal buoyancy parameter Magnetic parameter and stretching sheet parameter. But an opposite trend is observed with an increase in the thermal buoyancy and radiation and permeability parameters.
2. It is found that temperature decreases with an increase in the Prandtl number, thermal buoyancy parameter, and permeability parameter, where as an reverse trend is observed with an increase in the Eckert number, solutal buoyancy parameter, stretching sheet parameter, radiation parameter, Nb, Nt, γ.
3. Concentration decreases with an increase in Ec, R, Nt, γ or γ_1 where as an opposite trend is observed with increase in M, Nb, or λ.
4. Skin friction coefficient increases with an increase in the Ec or Nb or Le or λ and decreases with an increase in M,R, $R1^{-1}$, Pr, Nt, m, δ, Pr, γ or γ_1.
5. Nusselt number or Heat transfer rate rises with a rise in the Pr, Le , $\gamma_1$or λ and it falls with an increase in the M, R, $R1^{-1}$, Nt , m or δ, Ec , Nb or γ.
6. Mass transfer rate increases with an increase in the R, Ec, Pr, Nb, Le, γ or γ_1 or λ and decreases with in increases in the M, R, Nt, m or δ.

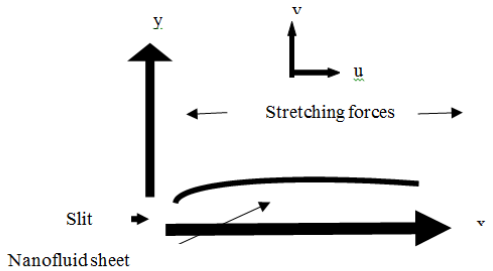

Fig. 1. A schematic model of the problem under consideration

BULLETIN OF MATHEMATICS AND STATISTICS RESEARCH
A Peer Reviewed International Journal,
Contents available on www.bomsr.com
RADMAS– 2016
Vol.4. S1.2016; ISSN: 2348-0580
Email:editorbomsr@gmail.com

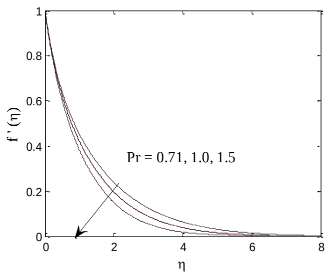

Fig. 2. Variations of velocity profiles for different values of Pr.

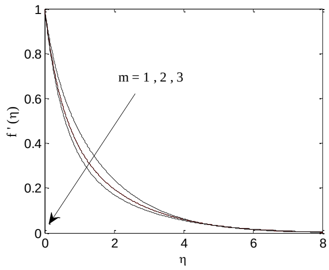

Fig. 3. Variations of velocity profiles for different values of m.

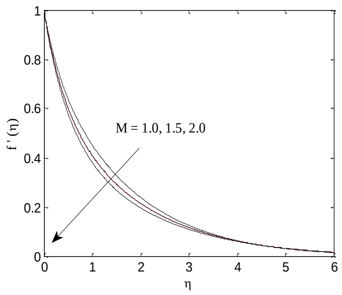

Fig. 4. Variations of velocity profiles for different values of M.

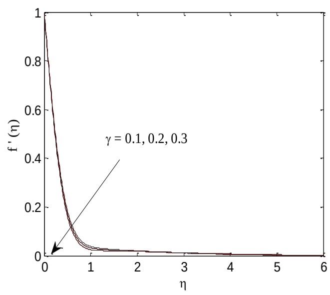

Fig. 5. Velocity Profiles for different Values of γ.

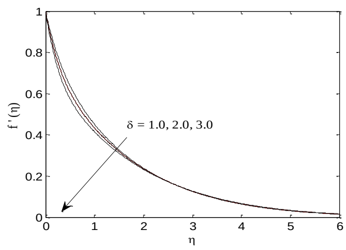

Fig. 6. Velocity Profiles for different values of δ.

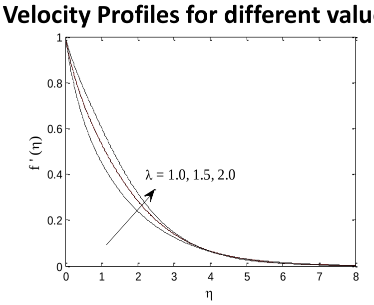

Fig. 7. Variations of velocity profiles for different values of λ.

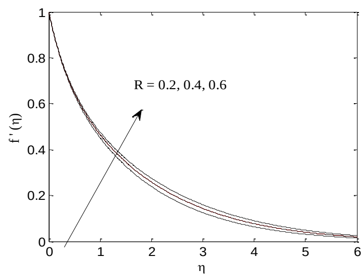

Fig. 8. Variations of velocity profiles for different values of R.

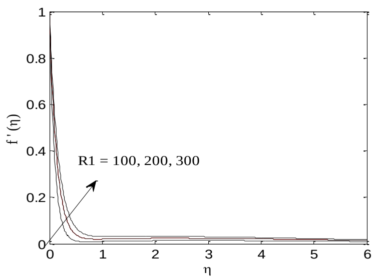

Fig. 9. Variations of velocity profiles for different values of $R1$.

BULLETIN OF MATHEMATICS AND STATISTICS RESEARCH
A Peer Reviewed International Journal,
Contents available on www.bomsr.com
Vol.4. S1.2016; ISSN: 2348-0580
Email:editorbomsr@gmail.com
RADMAS– 2016

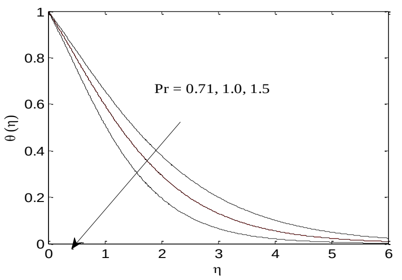

Fig. 10. Variations of temperature profiles for different values of Pr.

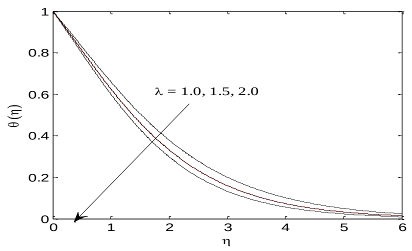

Fig. 11. Variations of temperature profiles for different values of λ.

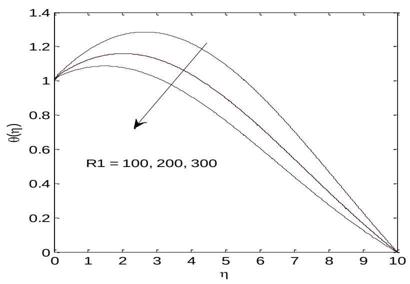

Fig. 12. Variations of temperature profiles for different values of $R1$.

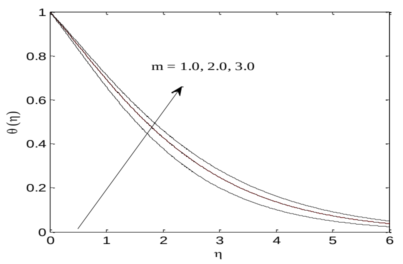

Fig. 13 .Variations of temperature profiles for different values of m.

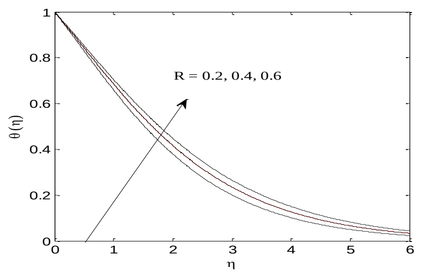

Fig. 14. Variations of temperature profiles for different values of R.

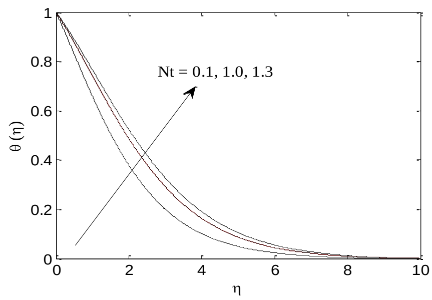

Fig. 15. Variations of temperature profiles for different values of Nt.

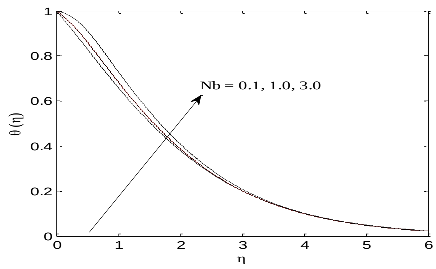

Fig. 16. Variations of temperature profiles for different values of Nb.

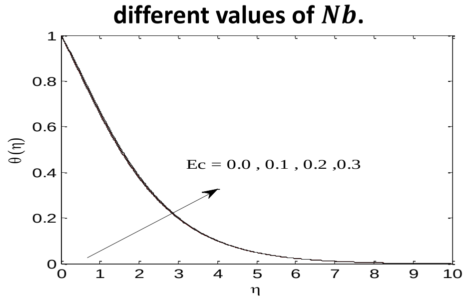

Fig. 17. Variations of temperature profiles for different values of Ec.

BULLETIN OF MATHEMATICS AND STATISTICS RESEARCH
A Peer Reviewed International Journal,
Contents available on www.bomsr.com
RADMAS– 2016
Vol.4. S1.2016; ISSN: 2348-0580
Email:editorbomsr@gmail.com

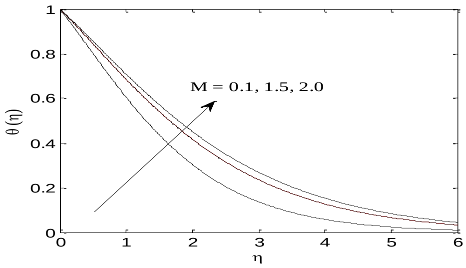

Fig. 18. Temperature Profiles for different values of M.

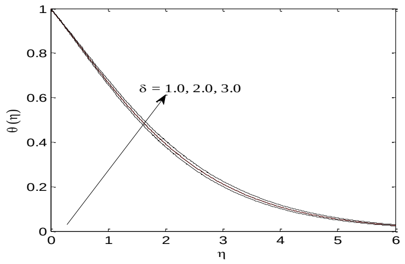

Fig. 19. Temperature Profiles for different values δ.

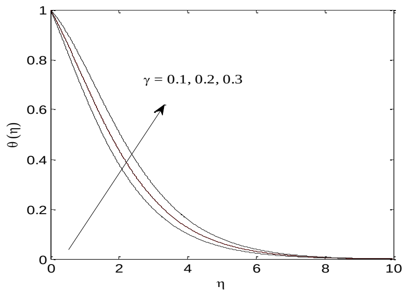

Fig. 20. Temperature Profiles for different values of γ.

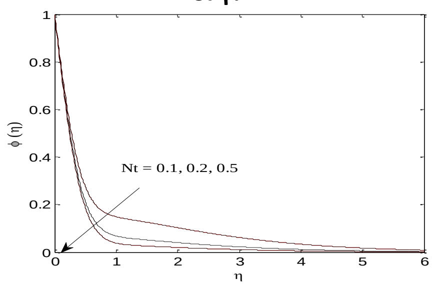

Fig. 21. Variations of concentration profiles for different values of Nt.

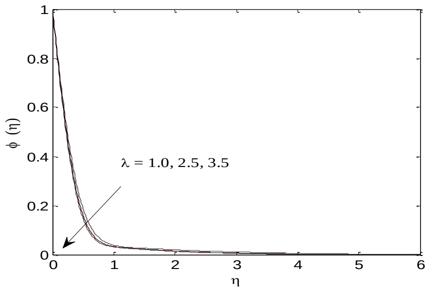

Fig. 22. Concentration profiles of different values of λ.

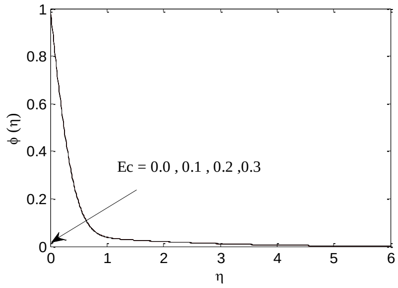

Fig. 23. Variations of concentration profiles for different values of Ec.

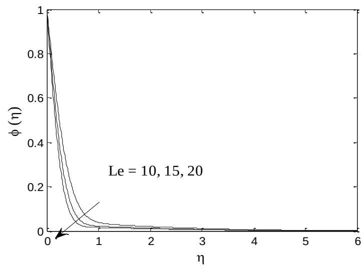

Fig. 24. Concentration Profiles for different values of Le.

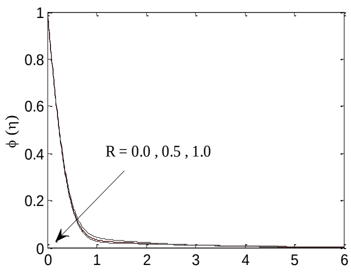

Fig. 25.Concentration Profiles for different values of R.

BULLETIN OF MATHEMATICS AND STATISTICS RESEARCH
A Peer Reviewed International Journal,
Contents available on www.bomsr.com
Vol.4. S1.2016; ISSN: 2348-0580
Email:editorbomsr@gmail.com
RADMAS– 2016

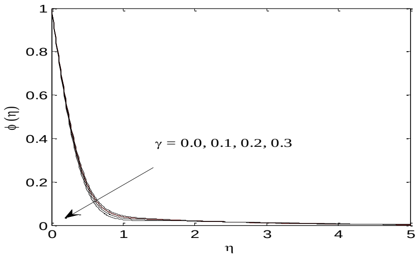

Fig. 26. Concentration Profiles for different values of γ.

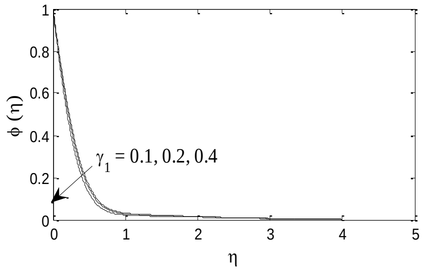

Fig. 27. Concentration Profiles for distinct values of γ_1.

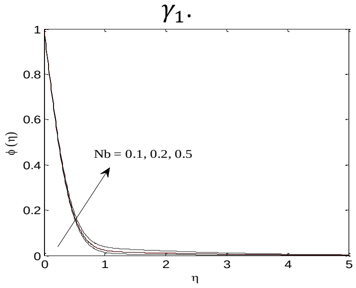

Fig. 28. Variations of concentration profiles for different values of Nb.

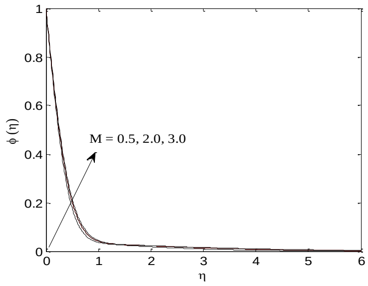

Fig. 29. Concentration Profiles for distinct values of M.

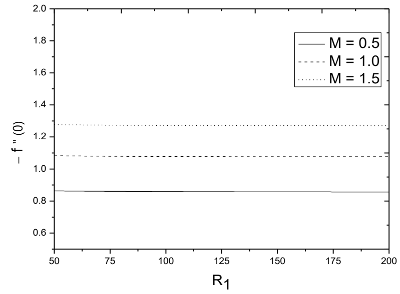

Fig. 30. Variation of the skin friction coefficient with M for different values of R_1.

ACKNOWLEDGEMENTS
The authors wish to express sincere thanks to the honorable referees for their valuable comments and constructive suggestions to improve the quality of the paper.

REFERENCES

[1]. Ahmad, S. and I. Pop (2010). Mixed convection boundary layer flow from a vertical flat plate embedded in a porous medium filled with Nanofluids. International Communications in Heat and Mass Transfer. 37, 987– 991.

[2]. Anwar, M.I., I. Khan, Sharidan S. and M.Z. Salleh (2012). Conjugate effects of heat and mass transfer of nanofluids over a nonlinear stretching sheet. International Journal of Physical Sciences. 7(26), 4081–4092.

[3]. Aziz, E.I. (2009). Radiation effect on the flow and heat transfer over an unsteady stretching sheet. Int. Commu. Heat and Mass Transf. 36, 521–524.

[4]. Brewster, M.Q, (1992). Thermal radiatiative transfer and properties. John Wiley. New Work.

[5]. Buongiorno, J. (2006). Convective transport in nanofluids. ASME J. Heat Transfer, 128, 240–250.

BULLETIN OF MATHEMATICS AND STATISTICS RESEARCH
A Peer Reviewed International Journal,
Contents available on www.bomsr.com
RADMAS– 2016
Vol.4. S1.2016; ISSN: 2348-0580
Email:editorbomsr@gmail.com

[6]. Buongiorno, J. and Hu (2005, May). Nanofluid coolants for advanced nuclear power plants, Paper no. 5705. proceeding of ICAPP'05, Seoul, 15- 19.

[7]. Cebeci,.T. and P.Bradshaw (1988). Physical and computational aspects of convective Heat Transfer, Springer Verlag, New York.

[8]. Cheng, P. and W. J. Minkowycz (1977). Free convection about a vertical flat plate embedded in a porous medium with application to heat transfer from a dike. Journal of Geophysical Research, 82, 2040–2044.

[9]. Choi, S.U.S. (1995). Enhancing thermal conductivity of fluid with nanoparticles, developments and applications of non–Newtonian flow. ASME FED, 231. 99–105.

[10]. Das, S.K, Putra, N. Thiesen, P. and W.J. Roetzel (2003). Temperature dependence of thermal conductivity enhancement for nanofluids.Heat Transfer. 125, 567- 574.

[11]. Fazlul Kader Murshed, Indranil Roychowdhary, Arnab Chattopadhyay (2015). Radiation effect of boundary layer flow of a nanofluid over a nonlinearly permeable stretching sheet. Advances in Physics Theories and Applications 40 43-54.

[12]. Gbadeyan, J.A, M.A. Olanrewaju and P.O. Olanrewaju (2011). Boundary layer flow of a nanofluid past a stretching sheet with a convective boundary condition in the presence of magnetic field and thermal radiation. Australian Journal of Basic and Applied Sciences, 5(9): 1323–1334.

[13]. Gnaneswara Reddy, M. (2014) Thermal radiation and chemical reaction effects on MHD mixed convection boundary layer slip flow in a porous medium with heat source and ohmic heating. Eur. Phys. J. Plus. 129, 41.

[14]. Gnaneswara Reddy, M (2014). Influence of thermal radiation, viscous dissipation and hall current on MHD convection flow over a stretched vertical flat plate. Ain Shams Eng J; 5:169–75.

[15]. Gnaneswara Reddy, M., P. Padma,and B.Shankar (2015). Effects of viscous dissipation and heat source on unsteady MHD flow over a stretching sheet. Ain Shams Eng J.04.006.

[16]. Hady, F.M, F.S. Ibrahim, S.M Abdel-Gaied and R.Eid. Mohamed (2012). Radiation effect on viscous flow of a nanofluid and heat transfer over a nonlinearly stretching sheet. Nanoscale Research Letters. 7, 229.

[17]. Haile, E. and B. Shankar (2014). Heat and mass transfer through a porous media of MHD Flow of nanofluids with thermal radiation, viscous dissipation and chemical reaction effects. Am Chem. Sci. J; 4, 828–46.

[18]. Jat, R.N and Gopi Chand (2013). MHD flow and Heat transfer over an exponentially stretching sheet with viscous dissipation and radiation effects. Applied mathematical Sciences, 7 4. 167-180.

[19]. Keller, H.B. (1992). Numerical methods for two point boundary value problems. Dover publications. New York.

[20]. Keller, H.B, (1974). Accurate difference methods for non-linear two point boundary value problems. SIIM J Num Anal. 11:305–20.

BULLETIN OF MATHEMATICS AND STATISTICS RESEARCH
A Peer Reviewed International Journal,
Contents available on www.bomsr.com
Vol.4. S1.2016; ISSN: 2348-0580
Email:editorbomsr@gmail.com
RADMAS– 2016

[21]. Khan, W.A, and I. .Pop (2010). Boundary layer flow of nanofluid past a stretching sheet. Int J Heat Mass Transf. 53: 2477 – 2483.

[22]. Kuznetsov, V.A, and D.A. Nield (2010). Natural convective oundary layer flow of a nanofluid past a vertical plate. International Journal of Thermal Sciences, 49(.2), 243 – 247.

[23]. Makinde, O.D. and P.O. Olanrewaju (2010). Buoyancy effects on thermal boundary layer flow over a vertical plate with a convective surface boundary condition. .J.Fluids Eng. Trans. ASME, 132: 044502- 1- 4.

[24]. Nadeem, S. C. and C. Lee (2012). Boundary layer flow of nanofluid over an exponentially stretching surfacve Nanoscale Res Lett , 7:94

[25]. Nield, D.A. and A.V. Kuznetsov, (2009). The Cheng-Minkowycz problem for natural convective oundary layer flow in a porous medium saturated by a nanofluid. International Journal of Heat and Mass Transfer, Vol. 52, no. 25 – 26, 5792 – 5795.

[26]. Olanrewaju, P O, Olanrewaju, M A and A O, Adesanya (2012). Boundary layer flow of nanofluids over a moving surface in a flowing fluid in the presence of radiation. .International Journal of Applied Science and Technology, 2, 274-285.

[27]. Rana P and R. Bhargava (2012) Flow and heat transfer of a nanofluid over a nonlinearly stretching sheet; a numerical study; Commun. Nonlinear Sci. Numer. Simulation, 17(1): 212 – 226.

[28]. Rohana Abdul Hamid, NorihanMd, Arifin, Roslinda Mohd Nazar, and loan Pop (2011). Radiation effects on Marangoni boundary layer flow past a flat plate in nanofluid, Proceedings of the International Multiconfernce of Engineers and Computer Scientists, Vol II, Hongkong.

[29]. Sandeep, N. and C. Sulochana (2015). Dual solutions of radiative MHD nanofluid flow over an exponentially stretching sheet with heat generation/absorption. Applied Nanoscience 5 (25).

[30]. Sib Sankar Manna, Sanatan Das and Rabindra Nath Jana (2012), Effects of radiation on unsteady MHD free convective flow past an oscillating vertical porous plate embedded in a porous medium with oscillating heat flux. Advances in Applied Science Research, Pelagia Research Library. 3(6), 3722 – 3736.

[31]. Singh P, Jangid A, Tomel NS, Sinha D (2010).Effects of Thermal radiation and magnetic field on unsteady stretching permeable sheet in presence of free stream velocity. Int. J. Info. And MathSci6(3),63-69.